New ground motion data and concepts in seismic hazard analysis

John G. Anderson*, James N. Brune, Rasool Anooshehpoor and Shean-Der Ni

Seismological Laboratory, MS 174, University of Nevada, Reno, Nevada 89557, USA

The strong motion data from the Izmit, Turkey and Chi-Chi, Taiwan earthquakes have pointed out uncertainties in current strong motion attenuation curves for large earthquakes. Although the near-source strong motion data from these two well-recorded large earthquakes were well below the estimated values by the ground motion models, they were consistent with constraints estimated from precarious rock methodology. This discrepancy could be a result of inadequate ground motion data for large earthquakes and possible flaws with a number of statistical parameter assumptions that were necessary for extrapolation from existing database, which is dominated by small earthquake data. This review article discusses several important issues that have the potential to cause major impact on seismic hazard analysis. They are: (i) partitioning of uncertainties into aleatory and epistemic contributions, (ii) quantification of precarious rock observations and use of the data to constrain and improve ground motion models, (iii) continuing to deploy strong motion instruments near major faults since only more strong motion data will definitively resolve the issues of what is normal behaviour, and (iv) understanding through modelling and observations, the physical phenomena that affect strong motion, including the effect of total fault offset, surface rupture and type of faulting.

Introduction

SEISMIC hazard analysis as developed over the past couple of decades has estimated both the possibilities and probabilities of seismic ground shaking of a given level based on identification of active faults, estimation of their associated seismicity and prediction of the probable consequent ground motions. Because of lack of ground motion data for large earthquakes, which dominate in seismic hazard, a number of statistical parameter assumptions were necessary for extrapolation from the existing database. Unfortunately the current database is not adequate to check these assumptions. Three recent developments provide impetus for a new evaluation of the situation: (i) the occurrence of two large earthquakes in regions of modern seismic instrumentation (Turkey and Taiwan), (ii) development of a methodology for using precariously balanced rocks to place constraint on ground motion which could have occurred at certain places in the last few thousand years, and (iii) new results from physical and numerical modelling, which suggest important characteristics of near-source ground motion for different types of faulting (thrust, strike-slip and normal). This article gives our current evaluation of the implications of these developments.

*For correspondence. (e-mail: jga@seismo.unr.edu)

Probabilistic and scenario seismic ground motions

Earthquake hazards can be analysed with both probabilistic and 'deterministic' methods. The probabilistic seismic hazard analysis (PSHA) maps and related products are important in assessing risks statistically. Uses for PSHA maps include seismic zonation for building codes, earthquake insurance and special studies for critical facilities. The latter class is best designated as 'scenario' methods. Scenario ground motions are estimated ground motions expected from a subset of the possible earthquakes, some of which may be made of just one earthquake. These can be contoured on maps, to portray a median estimate of ground motions from events that are reasonable, and often regionally cause the most significant hazards. The intent is that the scenario map answers the common question: 'If the . . . fault ruptures, what do you expect?' Uses for scenario maps include educating the public about the earthquake hazards, some engineering applications and hazard response planning.

Probabilistic seismic hazard maps

One approach to presenting seismic hazard is by way of a probabilistic map. A probabilistic map[1–4] might contour, for instance, estimates of peak ground accelerations that occur with a probability of 10% in 50 years. Probabilistic maps thus communicate estimates of the relative hazards, accounting for both severity of the potential ground motions and their frequency of occurrence[5] and they provide a way to compare hazards of different locations in a scientifically justifiable and socially equitable way[6]. The USGS–CDMG probabilistic maps for the US that were developed by Frankel *et al.*[4] are a significant landmark for the description of seismic hazards in the US. Input for those maps was developed based on an extensive process

of soliciting expert advice and incorporating the best available information on local hazard sources.

The seismic hazard curve is the central concept for probabilistic maps. In principle, every specific site has its own seismic hazard curve. Curves for nearby sites are of course correlated. A hazard curve gives the average annual frequency at which some ground motion parameter is equalled or exceeded as a function of the amplitude of that parameter. Thus, hazard curves predict the result of an experiment where an instrument at the site records ground motions for, say, 10^5 or 10^6 years, and the frequency of excedence of the ground motion parameter is tabulated as a function of its amplitude. Milne and Davenport [7] presented a method to estimate the hazard curve at relatively high probabilities directly from a seismic catalogue, but most estimates synthesize earthquake sources and attenuation relations using an approach that can be traced to Cornell[1]. Map preparation requires estimation of hazard curves for a grid of points, and then contouring the selected parameter.

The Panel on Seismic Hazard Analysis[8] concluded that PSHA, 'when carried out with an appropriate level of sophistication to satisfy the needs of the user, can be regarded as an acceptable procedure for describing the seismic hazard.' The clause 'appropriate level of sophistication' is focused on the use of suitable techniques, which are believed to assure that hazard estimates are reliable at the probability level of concern. There are, of course, uncertainties involved in estimating hazard curves[9–11]. Nearly every aspect of strong motion and engineering seismology research[12] still has contributions to make for improving the input to PSHA. Thus the extent to which the PSHA results would agree with an empirical hazard curve, as described above, is not known.

Some recent research has focused on methods to test the output of a PSHA. This is a difficult task, since the part of the hazard curve that is most significant for engineering applications occurs where the PSHA attempts to estimate the rates of events with repeat times of hundreds to thousands of years. Ward[13] tested a southern California model at relatively high annual probabilities ($\sim 10^{-2}$) against a model derived using the Milne and Davenport[7] approach, with satisfactory agreement. Southern California and Nevada models have been tested by Brune[14] and Anderson and Brune[15], respectively, at smaller annual probabilities ($\sim 10^{-4}$), estimated from observations of old precariously balanced rocks. There are some contradictions. The sections below summarize some new tests and their emerging importance.

Scenario seismic hazard maps

Another type of map for displaying seismic hazard is commonly called 'deterministic' (e.g. refs 16 and 17) or maps of ground motions based on 'maximum credible earthquakes' (e.g. ref. 18). These maps contour ground motions expected from a selection of earthquakes that could happen in the region. For instance, Mualchin[18] identifies large but plausible earthquakes on every active fault and then estimates ground motions from each. Then the largest of these values for each grid point on the map is contoured. Additional examples of 'deterministic' maps are available for California[19,20] and Nevada[21,22]. While he made no effort at completeness, Nuttli[23] applied this concept and produced a widely used map that clearly and simply communicates that seismic hazards affect much of the US. The approach seems conceptually direct, and is easily understood by scientists and non-scientists alike.

Although the 'deterministic' label is deeply embedded in the literature, for several reasons Anderson[24] suggests that results of this procedure should be called 'Scenario Ground Motions'. The scenario is the central concept for the 'deterministic' or 'maximum credible earthquake' seismic hazard maps. Reiter[16] defines 'deterministic analyses' as 'those which, for the most part, make use of discrete, single-valued events or models to arrive at scenario-like descriptions of earthquake hazard'. The American Heritage Dictionary of the English Language defines the term 'scenario' as 'an outline or a model of an expected or a supposed sequence of events'. The term also carries the connotation that the imagined sequence is one of several possibilities. Thus a scenario earthquake is some large event that is believed to be possible on an active fault identified by geologists, and its selection process allows regional flexibility and judgement.

Planning scenarios are an excellent way to communicate seismic hazards, and their consequences, to a wide audience[25–27]. In addition, the FEMA programme HAZUS, uses the scenario as a basis for its estimates of earthquake losses. Typically, a planning scenario begins with a description of faulting and possible ground motions from some selected event for a region. The event is selected because it is one of the most severe that could affect the region. The extent of rupture and inferred magnitude needs to be scientifically reasonable, but the presence of judgement is implicit in the term 'scenario'. There is no pretence that the scenario earthquake is uniquely defined. It is also understood that the effects of the earthquake are not particularly sensitive to uncertainties on the magnitude. In some cases, the planning scenario earthquakes have a very low probability. Nonetheless, they are useful for emergency planning and critical engineering designs for public safety, in that they communicate some rather severe but plausible ground motions. By preparing for such a case, planners and engineers can be relatively confident (but not certain) that they have done what they can to prepare for any earthquake event.

Comparison of probabilistic and scenario maps

The scenario maps generally show ground motions from a subset of earthquakes that, based on judgement, cause the

greatest regional concern. Unlike a probabilistic description, scenario maps do not explicitly incorporate the frequency of occurrence of the earthquakes, and thus the maps are not sensitive to uncertainties on occurrence rate. The scenario approach does implicitly use information about earthquake rates in the selection of the events that are on the maps. Scenario maps and probabilistic maps complement each other in presenting the seismic hazard, in that they communicate different information. However, scenario maps can be made even more useful if the added information about activity rates is also presented.

The ergodic assumption in probabilistic seismic hazard maps

An ergodic process is a random process in which the distribution of a random variable in space is the same as the distribution of that same variable at a single point, when sampled as a function of time. An ergodic assumption is commonly made in PSHA. A regression analysis is used to obtain a mean curve to predict ground motion as a function of magnitude and distance (and sometimes other parameters). The standard deviation of this ground motion regression is determined mainly by the misfit between observations and the corresponding predicted ground motions at multiple stations for a small number of well-recorded earthquakes. Thus, the standard deviation of the ground motion regression is dominated by the statistics of the spatial variability of the ground motions. An ergodic assumption is made when PSHA treats spatial uncertainty of ground motions as an uncertainty over time at a single point[28,29]. The basic elements of probabilistic seismic hazard analysis were formulated by Cornell[1]. They are summarized in the context of the ergodic assumption[29] wherein it is shown that at least in specific idealized cases, the use of the ergodic assumption overestimates ground motion when exposure times are longer than earthquake return times.

The motivation for examining the effects of the ergodic assumption comes from several studies of precarious rocks. Brune[14] found that the distribution of precarious rocks in Southern California is not consistent with the large values of ground motion predicted by PSHA studies. Similarly, Anderson and Brune[15] concluded that most of the known precarious rocks in Nevada are inconsistent with the PSHA maps of Siddharthan *et al.*[22]. In southern California, the distribution of precarious rocks is reasonably consistent with the hazard maps of Wesnousky[30]. Anderson and Brune[29] point out that for the sites in the Mojave Desert, the controlling difference between the PSHA maps and the maps of Wesnousky was that the latter used only the median value for attenuation of peak ground acceleration with distance, whereas the PSHA maps added a statistical (Gaussian) uncertainty to the ground motion[3], utilizing the ergodic assumption. These observations suggest the need for a more detailed look at the way the probabilistic seismic hazard is estimated.

The ergodic assumption and partitioning of uncertainty into epistemic and aleatory parts

Some PSHA now distinguish between aleatory and epistemic uncertainty. Aleatory uncertainty is introduced by true randomness in nature, while epistemic uncertainty is due to lack of knowledge. The definition and separation of aleatory and epistemic uncertainty has been articulated most extensively by the Senior Seismic Hazard Analysis Committee (SSHAC)[32], which regarded their division to be model-dependent and sometimes arbitrary. In their view, a model with a small number of variables, which is desirable from a practical viewpoint, will have a larger aleatory uncertainty than a model that uses more parameters. For instance, they suggest that adding more parameters to describe the path and site increased epistemic uncertainty, but reduced aleatory uncertainty since the ground motion should be predicted better if all of those parameters are described correctly.

The Panel on Seismic Hazard Evaluation[33] which has reviewed the views of SSHAC also considers that the division between aleatory and epistemic uncertainty is model-dependent, somewhat arbitrary and ambiguous. Both these panels seem to accept that the mean hazard does not depend on how much of the total uncertainty is aleatory and how much is epistemic. The main advantage of the separation however is to help experts formulate the input to the PSHA and to advise decision-makers of the potential future volatility of the mean hazard.

Anderson and Brune[29] reviewed the elements of PSHA and the recommendations of SSHAC. They propose that it is of critical importance to distinguish between aleatory and epistemic uncertainties in a probabilistic seismic hazard analysis, as this treatment contains the necessary elements for a solution to the problem introduced by the ergodic assumption. We reproduce, in Figure 1, the results of PSHA for a simple case in which all of the hazard comes from a single fault, to illustrate the opposite results of assuming all uncertainty is aleatory or assuming all uncertainty is epistemic. Ground motions are assumed to be due to characteristic ground motion earthquakes[29] defined as 'an earthquake which is first a characteristic earthquake and which furthermore is dynamically the same every time so the ground motion time history at a site near the fault is identically repeated'. Because each earthquake is dynamically identical, the ground motion at the site should be the same for every event. Thus, the hazard curve is a step function suggesting that the peak acceleration will occur for ground motions less than some value and that the probability that it will occur for larger ground motions is zero. Because we may not know before the record of the next earthquake what that ground motion

will be, there are different possibilities for this curve as illustrated in Figure 1. The conclusion from this figure is that these contrasting treatments can make an important difference in the results of PSHA.

The development by Anderson and Brune[29] presents an absolute standard for the definition of the aleatory uncertainty. Because of the way it enters the analysis, it should only describe the variability of the ground motion parameter over time, and should originate only from changes in the source when there are repeated realizations of similar events on the same fault. Since the path is identical in such events, its effect is predictable and the corresponding uncertainty is therefore epistemic. If path and site factors play a major role, as is generally believed, a major fraction of the uncertainty is epistemic (due to lack of knowledge of the role they play). In the use of the ergodic assumption in a basic seismic hazard analysis, all of this uncertainty is treated as aleatory.

This raises the issue of how the total uncertainty should be divided into the aleatory and the epistemic contributions. Anderson and Brune[29] discussed various considerations. The basic elements to consider follow. If the total uncertainty is σ_T, the aleatory uncertainty is σ_A, and the epistemic uncertainty is σ_E, then the uncertainties are related by:

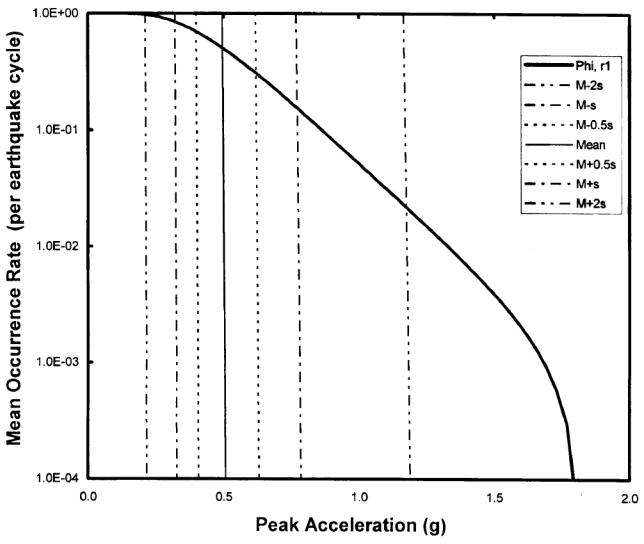

Figure 1. PSHA for a simplified case in which all of the hazard comes from a single fault which fails repeatedly in characteristic ground motion earthquakes, to illustrate the effects of the ergodic assumption. As in any PSHA, this gives hazard curves giving the mean occurrence rate of a ground motion (peak acceleration in this case). For clarity, the mean occurrence rate is given in repetitions per earthquake cycle, rather than per year as is normally done. The heavy line, (phi) gives the result for a PSHA in which all of the uncertainty on the ground motion is treated as aleatory. The near-vertical lines represent the results of a PSHA in which all of the uncertainty is treated as epistemic. It is not known which of the vertical hazard curves to choose, but that weighting does not depend on the exposure time and thus the overall estimate of hazard also does not depend on exposure time.

$$\sigma_T^2 = \sigma_A^2 + \sigma_E^2.$$

For a typical regression for peak acceleration, where the ground motion prediction equation gives the natural log (i.e. base e) of peak acceleration, σ_T is typically about 0.50. Relative to the regression model by Abrahamson and Silva[34], the maximum aleatory uncertainty consistent with the precarious rocks is site-dependent[31], but is never much more than 0.3 (natural log units) and at some sites must be less than about 0.1. For multiple realizations of a synthetic model[35], the uncertainty due to the source is typically about 0.2. If this reasoning is realistic, the epistemic uncertainty would be dominant, but the aleatory part would not be negligible. The distribution of uncertainty between the aleatory and the epistemic parts need to be resolved by data, not by assumption[29], and is a difficult problem to solve due to limited data.

Since it is standard practice in PSHA to treat most of the uncertainty in ground motion as aleatory[4,22,36], many hazard maps may end up with different ground motions at low probabilities if the uncertainties are redistributed between aleatory and epistemic.

Parameterization of ground motion

A critical input to the seismic hazard analysis is the ground motion model. This can be done in different ways. For the probabilistic studies, the usual type of input is various ground motion parameters predicted using regression equations. Examples of these ground motion prediction equations exist for a variety of tectonic environments[34,37–43]. Scenario maps will generally use the same ground motion prediction equations.

Two recent studies have looked at the general problem of characteristics expected from ground motion prediction equations. Anderson[44] concluded that the expected shape for peak acceleration on rock as a function of magnitude and distance changes as the magnitude increases. Specifically, the ground motion at short distances does not increase as rapidly as at large distances. This is a consequence of the interaction of two effects. Firstly, as magnitude increases, the source dimension and consequent duration for wave radiation increases, with the effect becoming very important above about magnitude 6. Secondly, as the distance increases, the dispersion and multipathing of seismic waves increases the duration of the Green function. Consequently, at large distances, early waves from a late part of the rupture combine statistically with the late waves from an early part of the rupture to increase the amplitudes. At short distances, this interference is less important due to the shorter durations of the Green's functions. Another study on the expected characteristics of ground motion prediction equations examined the expected effect of nonlinear soil response on the ratio of ground motions on soil and rock[45]. This builds on seve-

ral recent studies that have recognized, in the seismological data from the large earthquakes, that nonlinear soil response is a common phenomenon[46,47]. Su *et al.*[48] concluded that in the Northridge earthquake, nonlinearity is recognizable in differences between site response (defined by spectral ratios) when peak acceleration exceeds about 0.3 g, peak velocity exceeds 20 cm/s, or peak strain exceeds 0.06%.

A series of studies on empirical ground motion models in southern California has recently been completed[49–55]. The focus was on improving probabilistic seismic hazard analysis through incorporation of site effects. Residuals grouped using one particular mapping of quaternary geology units[56] and relative to one ground motion model did not yield statistically significant correlations[53], but a grouping of geological units by near surface velocity in the upper 30 m (ref. 57) did result in improved predictions[50]. This suggests that when incorporating surface geophysics, some amount of trial and error may be necessary to take advantage of careful geological mapping. Another result of this project is the demonstration that ground motion residuals depend on the depth of the sediments at the site[50,53,55]. Basin depth was defined as the depth to the interface with material with a shear velocity of 2.5 km/s, based on a 3D velocity model[58]. Basin depth may be a proxy for some other parameter[49], such as distance from a basin edge[59] or average 3D basin effects at low frequencies[54]. The 3D basin effects calculated at low frequencies are in fact, highly dependent on the source location and even the source dynamics in some cases[54], indicating that the average response has a considerable amount of variability. The total effect of incorporating these parameters to represent site response into regressions does not reduce the uncertainty in ground motions by a very significant amount[52,60].

Detailed studies of the seismic hazard at specific sites are increasingly using scenario ground motions that consist of complete synthetic seismograms, particularly when an appropriate historical record from an equivalent situation is not available. Various studies have demonstrated that synthetic seismograms are capable of reproducing the statistical characteristics of strong ground motions[35,61]. We do not review the developments in this field here, except to note that it is a rapidly growing subject driven by the engineering needs to have seismograms, not available in the empirical data set, that represent the event size, source geometry, regional wave propagation to the specific distance of engineering interest, and site conditions appropriate for specific sites.

New strong motion data from the Turkey and Taiwan earthquakes

In the second half of 1999, two earthquakes contributed significantly to our understanding of strong ground motions. The first was the M_W 7.6 earthquake on 17 August 1999, which struck western Turkey. The second was the M_W 7.6 earthquake on 21 September 1999 that struck central Taiwan.

A preliminary overview of the Kocaeli, Turkey earthquake is given by the US Geological Survey[62]. The mechanism for the earthquake was right-lateral strike slip. There were approximately 38 strong motion recordings of this earthquake. Anderson *et al.*[63] estimated the site conditions and carefully measured the locations for the nearest stations. Figure 2 compares the peak acceleration recorded at the four nearest rock stations with the predictions of four ground motion models. As peak acceleration is an indicator of the high-frequency content of the accelerograms, this figure demonstrates that the high-frequency content of this earthquake was overestimated by the ground motion models.

The strong motion programme in Taiwan and preliminary results for the Chi-Chi, Taiwan earthquake, are summarized by Shin *et al.*[64]. The Chi-Chi earthquake had a thrust-faulting mechanism on a fault with an average dip of 25 degrees, and caused surface rupture over a zone about 80 km long[65]. Taiwan is very densely instrumented, and the earthquake occurred near the centre of the island, resulting in virtually every operating instrument on the island being triggered. A preliminary data release by the Central Weather Bureau contains traces for 422 accelerograms for the main shock.

Figures 3 and 4 show the peak accelerations from the Chi-Chi earthquake compared with ground motion predic-

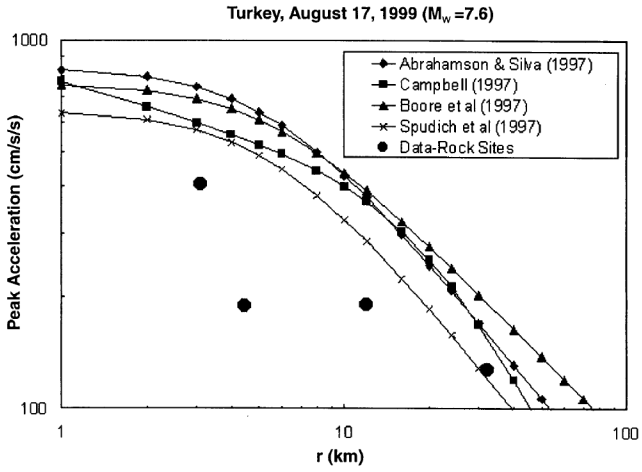

Figure 2. Peak accelerations from the 17 August 1999 earthquake in Turkey (M_w 7.6) compared with four different ground motion models (from Anderson *et al.*[63]). Peak accelerations are for sites that would be dominated by erosion based on local topography. For that reason, Anderson *et al.* concluded that the underlying geology would at most have a thin layer of soil formation over bedrock, and they classified these sites as rock sites. Anderson *et al.*[63] measured the station locations and the nearby fault locations using a handheld GPS receiver, and thus the distances are accurate to better than 100 m in most cases. The distance to the fault located here at about 12 km is uncertain due to questions on where the fault ruptured under the Sea of Marmara; the distance plotted here is an upper limit (from Anderson *et al.*[63]).

tions. The site conditions are not known for all the stations on these figures, so the peak accelerations are compared with both soil and rock ground motion models. The results are the same for both models: the observed peak accelerations are smaller than those predicted by the models.

Effect of Turkey and Taiwan data on attenuation curves

The Turkey and Taiwan earthquakes are the first major continental earthquakes to be extensively recorded at very short distances. It is therefore a significant puzzle to explain why the peak accelerations are overestimated by the ground motion models for both earthquakes. We discuss some alternatives. All of the alternatives fall into two categories: those that consider that the 1999 earthquakes are representative of earthquakes of their size and setting, and those that would consider the earthquakes anomalous.

The arguments that would favour that these earthquakes are anomalous would mainly be based on past experience: the ground motion models are based on some data, although it is sparse. The 1992 Landers earthquake (M 7.2, strike-slip mechanism) generated one record (1.1 km from the surface rupture) near a part of the fault with significant fault slip, and the peak horizontal accelerations on that record were higher (700 and 784 cm/s/s)[66]. The 1940 and 1979 Imperial Valley earthquakes also produced large peak accelerations near the fault. The 1952 Kern County earthquake (M 7.6, continental thrust mechanism) was recorded on four strong motion stations, and peak accelerations at all of those stations are near the upper edge of the cloud of points on Figure 3. A problem with this line of reasoning is that it is highly unsatisfying and unscientific, when one only has two well-recorded major continental earthquakes, to assume that both are anomalous.

The earthquakes that have generated higher ground motions in the past mostly have a smaller magnitude. One alternative to reconcile all of the data might be to abandon the assumption that is generally made in the regression analysis to develop ground motion models that the median peak acceleration is a monotonically increasing function of magnitude, for distance held constant. Some additional support for that hypothesis might be obtained from the data from the Guerrero, Mexico strong motion network. Anderson and Lei[67] and Anderson[68] fit a non-parametric surface through the abundant data from that network as an alternative to assuming a parametric shape. They used different degrees of smoothing in fitting the surface; it is interesting that in the surface where they smoothed the data the least, the peak acceleration surface peaked at magnitude about 7.0 at short distances, and decreased above there to the largest magnitude in the data: magnitude 8.1.

It is possible that all of the earthquakes are 'typical', but that the differences in the fault physics are what cause the peak accelerations to be low in the 1999 events. If that is the case, then one must seek a physical explanation for what differs in the 1999 events that caused them to be low. Paul Somerville[69] has suggested that the difference may have something to do with whether or not the rupture breaks the surface. He points out that there are high accelerations in several events that do not break the surface

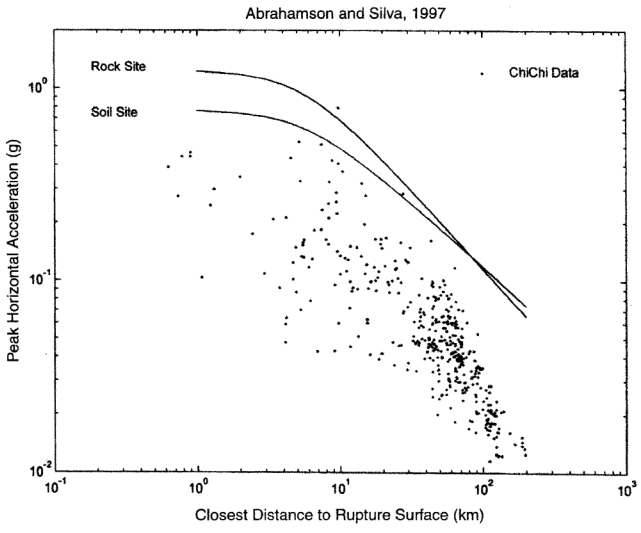

Figure 3. Peak accelerations from 21 September 1999 Chi-Chi, Taiwan earthquake (M_w 7.6) compared with the Abrahamson and Silva[34] ground motion models for rock and for soil site conditions. In this case, the site conditions are not known, but it is evident that in any case most of the points are significantly below the median prediction of the model regardless of site condition. Four points on this plot (identified in the figure) correspond to peak accelerations from the 1952 Kern County earthquake, which had a similar mechanism and magnitude.

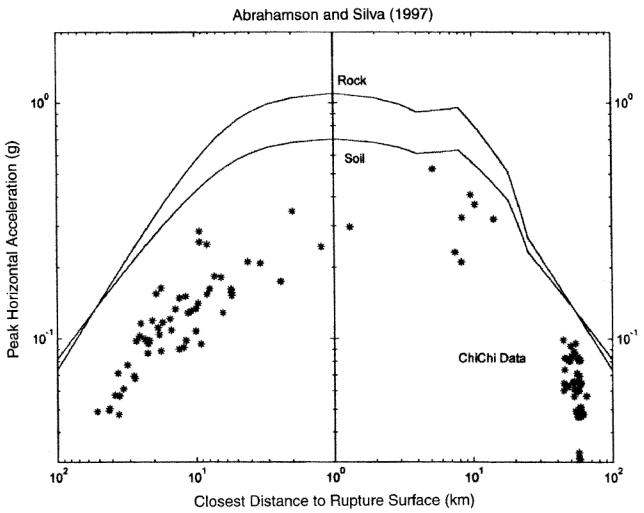

Figure 4. Like Figure 3, except for a subset of the data that comes from stations on an east-west cross-section across the fault. Points on the left hand side of the figure are on the footwall of the fault, and points on the right hand side are on the hanging wall. The Abrahamson and Silva[34] ground motion model distinguished between these two cases, as shown.

(e.g. Loma Prieta, Kobe, Northridge) and low accelerations in earthquakes that do break the surface (Chi-Chi, Kocaeli). A possible mechanism could be generation of high-frequency energy at the upper limit of the rupture.

An alternative model that we find particularly credible would have more to do with the history of rupture on the fault. Both the Kocaeli and Chi-Chi earthquakes occurred on major faults with tens to hundreds of kilometres of slip in previous earthquakes. The Landers and Northridge earthquakes occurred on faults with much less geological offset. The Loma Prieta earthquake occurred on a steeply-dipping oblique-thrust fault that may differ from the main San Andreas Fault in that area, so it also would appear to be in a category of faults with a smaller amount of total geological offset. The Mexican data also fit this pattern: the 1985 M 8.1 event was on the main subduction thrust, but the smaller events could have been located on shallower secondary thrust features. This hypothesis is motivated by the observations by Wesnousky[70] that faults with large geological offset tend to have straighter, more regular surface traces. The smoother surfaces generated by large offset would tend to have fewer irregularities to generate high frequency radiation than would a fault with less offset and thus less smoothing due to wear in large numbers of earthquakes.

The uncertainty in how to interpret the abundant data from the 1999 earthquakes points out the fundamental need for more data. It is essential that vigorous strong motion monitoring programmes continue near the major surface faults throughout the world. It would be completely unjustified to presume that the data from these two earthquakes (one strike-slip and one thrust) constitute an adequate sample of strong motions from earthquakes of this size.

Incorporation of various kinds of geological ground motion indicators into seismic hazard assessment

Status of precarious rock methodology

The importance of precarious rock studies in estimating seismic hazard has been given impetus by the following developments:

- Strong motion data from the Izmit, Turkey and Chi-Chi, Taiwan earthquakes discussed earlier, have pointed out the uncertainties in current strong motion attenuation curves for large earthquakes. Although the near-source strong motion data from those two earthquakes were considerably below the median for current attenuation curves (almost one standard deviation)[63,71], the data from these two earthquakes are consistent with constraints estimated from precarious rocks[15,63,72–74]. Thus the precarious rock evidence suggests that the attenuation curves assumed in the recent USGS–CDMG hazard maps give values which are too high at short distances, and thus may lead to serious overestimation of seismic hazard in some cases. Conversely, one could argue that the new data tend to give some limited support (only two large events) to published estimates from precarious rock studies.
- The precarious rock data near the San Andreas Fault in the Mojave Desert, where the seismic hazard is dominated by repeating large earthquakes on the San Andreas Fault, have pointed out a potentially important source of error in the current PSHA methodology, the so-called ergodic assumption discussed earlier, i.e. the assumption that for ground motion parameters (peak ground acceleration (PGA), or response spectrum values), the random variation in the time domain for repeated events with a given source-station configuration can be inferred from the scatter in space for individual events. The contrary extreme would be that, for a given source-station configuration, repeated events may have more or less the same rupture characteristics, and thus similar ground motion characteristics (the assumption of so-called 'characteristic ground motion earthquake'[15,72]). The ergodic assumption corresponds to one extreme method of dividing uncertainty between epistemic and aleatory uncertainty, and in fact represents the conservative extreme in which the assumed aleatory uncertainty is maximized[15,63]. At present the precarious rock methodology appears to be the only way to resolve this uncertainty, aside from waiting for a couple of dozen more large earthquakes to be recorded on strong motion networks, which may take many decades.
- The arbitrary assumption that median attenuation curves for large earthquakes must have a shape similar to that for smaller earthquakes, an assumption used in some regression analyses (see above), has been brought into question by precarious rock studies.
- The precarious rock methodology has been developed to the point that many of the initial skeptical concerns have been addressed in various publications[72,75–78]. No fundamental objections have been raised. The remaining uncertainties have to do mainly with the precision that can be obtained on ground motion constraints. These uncertainties can be addressed by improved field testing techniques, statistical numerical studies and shake table tests. Preliminary results from shake table tests have confirmed the preliminary estimates from previous studies[79].

Although the precarious rock methodology is still in an early stage, the above considerations and developments suggest that it may soon become accepted as a critical source of information for constraining PSHA maps. It has already led to opening up of discussion about several important assumptions commonly made in producing such

maps. In the conclusions we will give our evaluation of the implication of precarious rock studies for seismic hazard studies.

Physical and numerical modelling of important characteristics of near-source ground motion for different types of faulting

Recent fully dynamic physical modelling studies have suggested important variations and asymmetries in near fault ground motions for the thrust, strike-slip and normal faulting[80,81]. Many of these differences have been corroborated in numerical lattice, finite element and finite difference models[76,82–85]. Since the strong motion database for near-source ground motions is so limited, these studies are potentially very important, especially since the strongest ground motions occur near the fault trace. Many of the near-source features are not represented or poorly represented by dislocation theory, which has been in common use until recently. Here we consider some of the recent evidences for near-source characteristics of strong ground motion.

Evidence for strong asymmetry in ground motions during thrust faulting (intense hanging wall and low footwall motions)

Recent thrust faulting models, both physical and numerical, have indicated very high ground motions on the hanging wall and relatively low motions on the footwall[76,80,82,85]. This led Allen *et al.*[86] to re-examine evidence for intense ground motions on the hanging wall of the 1971 San Fernando earthquake. They concluded that an asphalt slab draped over the outcrop of the fault indicated that the asphalt had been nearly in free fall and the ground accelerations and velocities must have exceeded 1 g and 100 cm/sec, respectively. They cited evidence from the 1887 India earthquake[87], the 1971 San Fernando earthquake[88], and from the 1945 Mikawa earthquake[89] as further evidence supporting intense ground motions on the hanging wall of thrust faults. Brune[90] described shattered rock evidence on the hanging wall of thrust faults in Southern California as further supporting evidence of intense ground motions. On the other hand, the lack of shattered rock and the presence of precariously balanced rocks on the footwall of two thrust faults in Southern California (Banning and White Wolf Faults) indicate relatively low ground motions. This evidence indicated strong asymmetry in ground motions for thrust faults[73]. This could be of critical importance to estimating earthquake hazard from potentially large earthquakes in, for example, northern India, the Los Angeles Basin in the US, and elsewhere in the world.

Shattered rock on the hanging wall of thrust faults in Southern California

Evidence from road cuts and stream channels crossing thrust faults in Southern California provides support for intense hanging wall ground motions. Rocks in the hanging wall of thrusts of the San Gabriel frontal system, the Banning Thrust, The White Wolf Thrust and the Malibu Thrust all have a typical shattered appearance. The shattered rocks have a relatively small range of sizes (10–100 cm) of nearly equi-dimensional blocks with interblock open space and relatively little evidence of shearing and fault gouge. The shattered appearance seems consistent with the rocks having undergone a shock of high strain while under little gravitational or tectonic confinement (i.e. near the surface). The strain which the rock is exposed to is approximately proportional to the ratio of the ground velocity to the shear wave velocity. Thus strains on the hanging wall of the recent Chi-Chi Taiwan thrust fault earthquake[64] were about (5 m/sec)/(2 km/sec) $= 2.5 \times 10^{-3}$. Large strains must have also occurred in the hanging wall of the 1971 San Fernando earthquake, where estimated velocities were greater than 1 m/sec, and in the hanging wall of the 1897 Indian earthquake for which Oldham[87] reported ground velocities greater than 2 m/sec (ref. 86). Such large strains would be very likely to cause the shattered rock appearance reported here.

Precarious rock evidence of low ground motions on the footwall of the White Wolf and Banning Faults

In contrast to the evidence of intense hanging wall ground motions, the footwall of the Banning and White Wolf Faults have precariously balanced rocks, relatively steep cliffs and no indication of the 'shattered rock' appearance, thus indicating a relatively low upper bound on the ground motions which could have occurred in the last few thousand years[73,90].

White Wolf Fault: The north-east section of the White Wolf Fault, which ruptured in the large, *M* 7.6, Tehachapi, California earthquake of 1952, has a large footwall outcrop of granite. Geodetic studies of the earthquake[91–93] indicate 1 to 2 m of slip in the 1952 earthquake with the rupture reaching very near the surface. The actual surface breakage was ambiguous because of the existence of thick landslide deposits over the projected outcrop of the fault. There was clear evidence of intense ground motion on the hanging wall[94].

Perhaps surprising from the point of view of the size of the earthquake, and the strong evidence of intense shaking on the hanging wall, there is clear precarious rock evidence that the shaking on the footwall was relatively weak. Within 7 km of the trace of the fault on the footwall

there are numerous 'semi-precarious' rocks (definition of 'semi-precarious' as given by Brune[75], estimated toppling accelerations about 0.3–0.5 g for accelerograms with the shape of the El Centro record of the 1940 El Centro earthquake.

Banning Fault: The Banning Thrust has had a major earthquake in the last thousand years[95] and probably several in the Holocene. The crystalline rocks of the San Jacinto Block south of the Banning Fault are ideal for producing precarious rocks. This rock type extends from about 4 km from the fault to more than 20 km. The centre of the San Jacinto Block is far enough from both the San Jacinto and San Andreas Faults that the main contribution to the ground-shaking hazard is from the Banning Thrust.

Semi-precarious rocks (toppling accelerations of about 0.3–0.5 g, as defined by Brune[75] exist on the south side (footwall side) of the Banning Fault, starting at a distance of about 4 km. Farther south, at a distance of about 15 km there exist 'precarious' rocks (toppling accelerations of about 0.2–0.3 g). The approximate estimates of bounds on ground motion decrease from about 0.5 g at a distance of 4 km to about 0.3 g at a distance of about 15 km. These values are significantly lower than the USGS–CDMG 2% in 50 year hazard map values for this area, which vary from about 1.0 g to about 0.7 g in the same distance range.

Asymmetry of ground motion in thrust faulting

The shattered rock and precarious rock evidence cited above tends to confirm the suggestion from the physical and numerical modelling evidence that the ground motion on the footwall of major thrust faults is much lower than that for the hanging wall. This asymmetry is also consistent with values from the recent Chi-Chi, Taiwan earthquake of 1999, the best instrumented thrust earthquake in history, which recorded considerably smaller ground motions footwall side, even though the stations there were primarily on sedimentary fill, which would tend to amplify the motion (Figure 4). The asymmetry is also supported by steady state dislocation models[96,97] and by recent dynamic numerical models[76,82,85]. If this ground motion asymmetry is verified for thrust faults in general, it has important implications for seismic hazard from thrust faults.

Comparison with regression curves

Regression curves for peak ground acceleration from oblique thrust faulting indicate accelerations of about 0.6 g for an M 7.6 earthquake at a distance of 4 km and about 0.45 g at a distance of 15 km (ref. 41). For the hanging wall these values may be too low, considering the shattered rock evidence. For the footwall these values are clearly too high to be consistent with the preliminary estimations from precarious rocks. Abrahamson and Silva[34] considered hanging wall–footwall asymmetry and gave regression curves which indicated stronger shaking on the hanging wall than on the footwall (Figure 4), but the difference became zero at the fault trace and was not nearly as pronounced as suggested here on the basis of shattered rock and precarious rock evidence.

Evidence for variations in intensity of ground motion along strike-slip faults

Recent evidence from physical and numerical models has indicated that ground motion from extensional strike-slip earthquakes (strike-slip earthquakes in extensional regimes) may be much lower than for strike-slip faults with a large fault-normal compression[81,84,85]. The Ely and Day study[84] was a finite-difference simulation of the Brune and Anooshehpoor[81] physical model, and gave very similar results. Data from compressional strike-slip earthquakes and thrust faults dominate in the determination of regression curves for ground acceleration used in the USGS–CDMG probabilistic hazard maps, and thus these maps may be too high for extensional regimes.

One of the main physical reasons for expecting low accelerations for strike-slip faults in extensional regions may be the fact that in extensional regions, the fault-normal component of stress on the fault must approach zero near the surface because the lithostatic stress is zero and the tectonic stress is extensional[81,98]. Thus relatively little strain energy can be stored up at shallow depth near the fault trace. Preliminary evidence from reconnaissance surveys for precarious rocks has provided support for such low ground accelerations in extensional regions.

Precarious rock evidence from the Honey Lake strike-slip Fault

A spectacular zone of precarious rocks exists in the Fort Sage mountains, near (1–7 km distance) the strike-slip Honey Lake Fault Zone, California, interpreted to be the locus of a few to several major earthquakes in Holocene time[99], and thus strong evidence for low ground accelerations from a major strike-slip fault zone in an extending region. The appearance and geomorphic conditions of the rocks indicate they have been in precarious positions for thousands of years. More than 50 such rocks occur in a relatively small region. Some of the rocks are only one or two kilometres from the trace of the fault. Thus these rocks are a constraint on ground motion for the extensional strike-slip fault in the Honey Lake Basin. The pre-

carious rock evidence is consistent with the ground motion implications of the physical foam rubber modelling and the numerical modelling cited earlier, and also consistent with strong motion data from the recent Izmit, Turkey earthquake[63,100].

Precarious rock evidence from the San Jacinto Fault at the north-east end of Hemet Valley, near Beaumont, California

Another zone of precarious rocks associated with an extensional strike-slip zone occurs near Beaumont, California, a few km from the active San Jacinto Fault. A preliminary estimate of the toppling accelerations for these rocks is about 0.4 g at a distance of about 5 km from the San Jacinto Fault. Although these values are again consistent with accelerations recorded in the recent Izmit, Turkey earthquake[63], they are considerably lower than predicted by current regression curves for the historic M 7.0 San Jacinto Fault earthquake, and much less than indicated for the region by the USGS–CDMG 2% in 50 year hazard maps (about 0.5 g). These rocks provide a potentially critically important source of data to constrain ground motions for strike-slip faults in this extensional region, since they survived not only the 1899 and 1918 earthquakes, but also probably several other such earthquakes in the last few thousand years. This part of the San Jacinto Fault is at the north-east end of Hemet Valley, an extensional rhombochasm associated with a right step in the San Jacinto Fault, and near the north-west terminus of the rupture zone of the M 7 San Jacinto earthquake[101]. The San Jacinto Fault is one of the most active in Southern California, with a slip rate of about 1 cm per year, and thus likely has produced several large earthquakes during the time period represented by the precarious rocks. Thus this region has the potential to provide important constraints on ground motion for extensional strike-slip faults.

Implications of data from the recent Izmit, Turkey earthquake

As mentioned earlier, most current attenuation curves for large earthquakes at near distances are based on very little constraining data. In fact they are extrapolations from data belonging to smaller earthquakes at larger distance, a data set dominated by thrust faults and strike-slip faults in compressional regimes. Thus it is questionable how accurate they are for extensional strike slip regimes. The first rock site data for a large strike-slip earthquake at the distances of the precarious rocks in this study were provided by the recent M 7.4 Izmit, Turkey earthquake. The accelerations recorded at the sites Sakarya (SKR) and Izmit (IZT) were 0.42 g at a distance of 4 km and 0.23 g at a distance of 5 km, respectively. These values are significantly lower (almost one standard deviation) than the median values predicted by recent attenuation curves, and thus cast the validity of these curves into some question[63]. Of course, one earthquake does not provide a sufficient sample for final conclusions, but rather emphasizes the uncertainty associated with current attenuation curves.

Since the accelerations recorded at SKR and IZT are consistent with our preliminary estimates of constraints provided by precarious rocks near extensional strike-slip earthquakes, this brings up the suggestion that the section of the North Anatolian Fault near SKR and IZT may be an extensional strike-slip fault. It is at the edge of the Sea of Marmara, which has the appearance of an extensional basin. A final evaluation of the stress state on this section of the North Anatolian Fault awaits further study, but the situation suggests the importance of precarious rock studies to further constrain the ground motions from extensional strike-slip earthquakes, and to better understand the accelerations recorded at SKR and IZT.

Evidence for low ground motions on the footwall of normal faults

There are no strong motion accelerograms from the near-fault (distance < 3 km) footwall of major normal fault earthquakes. Recent physical and numerical models of normal faults indicate that the footwall has relatively low ground motions compared to similar strike-slip ruptures[76,82,83,102,103]. In the foam rubber model of Brune and Anooshehpoor[102], the ground motions on the footwall of a physical normal fault model were about 1/5 to 1/10 of those for strike-slip faulting (the same stress conditions but different rupture geometry – however, the difference is not so great if the strike-slip fault has a shallow weak layer[81]). The ground motions along the hanging wall were also low, but not as low as for the footwall. Preliminary observations of the distribution of precarious rocks on the footwall of normal faults supported the conclusion of very low footwall accelerations for normal faults[75], suggesting upper limits on ground accelerations of about 0.2 to 0.3 g (for a seismogram shape expected for large earthquakes, i.e. not a sharp, high frequency spike).

In stark contrast to earlier observations for strike-slip faults[75], observations of precarious rocks along major normal faults in California and Nevada show precarious and semi-precarious rocks extending nearly to the fault trace on the footwall side. Many precarious and semi-precarious rocks are observed within a few kilometres of the footwall of major normal faults, including the Pleasant Valley, NV; Carson City, NV; Genoa, NV; Antelope Valley, CA; and Owens Valley, CA faults. These are all known or believed to have had major earthquakes ($M \sim 7$–7.5) in

Holocene time (10 ka or younger). The Pleasant Valley Fault generated a large M_s 7.6 earthquake in 1915, the northern Genoa Fault generated a major earthquake, M 7+, about 600 years BP (ref. 104), the Carson City Fault generated a major earthquake about 500 years ago, possibly at the same time as the northern Genoa Fault earthquake[105]; the Antelope Valley Fault has a very young looking late Holocene scarp[106], and the Owens Valley Fault is shown as having a segment with Holocene rupture in the CDMG hazard map[107]. The young dates of these earthquakes make it essentially certain that the precarious rocks observed in this study survived the ground motions of large earthquakes. Recent revised attenuation curves for rock sites in extensional regions (SEA 99) give values about 10% higher near the fault[108]. Since there are no instrumental near-source (< 3 km) footwall accelerogram records for large normal faulting earthquakes, these curves have been extrapolated primarily from relatively large distance data from smaller normal fault earthquakes (e.g. ref. 109), or data from strike-slip earthquakes, and thus are quite uncertain. Since the new regression still does not include large magnitude-near source data, this difference is not significant. The precarious rock preliminary toppling accelerations[72] suggest an upper limit on ground motions that is considerably lower than the extrapolated mean empirical attenuation curves, supporting the thesis that the ground motion on the footwall side of normal faults is considerably less than that for strike-slip faults, as found for the foam rubber dynamic model of Brune and Anooshehpoor[102]. The values are also considerably lower than values from the recent USGS–CDMG seismic hazard maps for average recurrence times of about 2500 years (2% probability in 50 years) for the faults along the eastern Sierra Nevada Frontal Fault zone (typical values of 0.6–0.8 g (ref. 4)). The low accelerations for normal faulting discussed here may be a partial explanation for the discrepancy between probabilistic estimates of ground motion and precarious rocks in Nevada discussed by Anderson and Brune[15].

The precarious rock observations support the thesis of relatively low footwall ground motions for normal faults relative to strike-slip faults, as reported for a dynamic foam rubber normal fault model by Brune and Anooshehpoor[102]. Their model was an actual physical model with the same physical properties (medium properties and fault surface properties) as the model used earlier to study strike-slip and thrust faulting[110–112], and with a shallow weak layer[81]. Therefore if the dynamics involved in the foam rubber models are similar to those involved in real earthquake ruptures, we might expect low ground motions on the footwall of normal faults.

Conclusions

The studies reviewed above have identified several important physical phenomena that have not been incorporated into seismic hazard analysis. They indicate that much research remains to be done to test the hypotheses and to develop the new models into tools for engineering applications. The key issues that we see as needing attention are:

- Partitioning of uncertainties into aleatory and epistemic contributions.
- Quantification of seismic rock observations and use of the data to constrain and improve ground motion models.
- Continuing to deploy strong motion instruments near major faults, since only more strong motion data will definitively resolve the issues of what is normal behaviour.
- Understanding through modelling and observations the physical phenomena that affect strong motion, including the effect of total fault offset, surface rupture and type of faulting.

1. Cornell, C. A., *Bull. Seismol. Soc. Am.*, 1968, **58,** 1583–1606.
2. Algermissen, S. T., Perkins, D. M., Thenhaus, P. C., Hansen, S. L. and Bender, B. L., US Geology Survey Open File Report, 1982, 99, 82–1033.
3. McGuire, R. K. (ed.), *The Practice of Earthquake Hazard Assessment*, International Association of Seismology and Physics of the Earth's Interior, 1993.
4. Frankel, A., Mueller, C., Barnhard, T., Perkins, D., Leyendecker, E. V., Dickman, N., Hanson, S. and Hopper, M., National Seismic Hazard Maps, June 1996, US Department of the Interior, US Geological Survey, MS 966, Box 25046, Denver Federal Center, Denver, CO 80225, 1996.
5. Cornell, C. A., National Earthquake Ground Motion Mapping Workshop, September 1995.
6. Allen, C. R., *Earthq. Spectra,* 1995, **11**, 357–366.
7. Milne, W. G., and Davenport, A. G., *Bull. Seismol. Soc. Am.*, 1969, **59**, 729–754.
8. Panel of Seismic Hazard Analysis, Probabilistic Seismic Hazard Analysis, National Academy Press, Washington DC, 1988.
9. Krinitzsky, E. L., *Eng. Geol.*, 1993, **33**, 257–288.
10. Krinitzsky, E. L., *Eng. Geol.,* 1993, **36,** 1–52.
11. Krinitzsky, E. L., *Eng. Geol.*, 1995, **39**, 1–3.
12. Anderson, J. G., Seismology Supplement, US National Report to the International Union of Geology and Geophysics 1987–1990, 1991, pp. 700–720.
13. Ward, S. N., *Bull. Seismol. Soc. Am.*, 1995, **85,** 1293–1309.
14. Brune, J. N, *Bull. Seismol. Soc. Am.*, 1996, **86,** 43–54.
15. Anderson, J. G. and Brune, J. N., *Bull. Seismol. Soc. Am.*, 1999, **89,** 456–467.
16. Reiter, L., *Earthquake Hazard Analysis*, Columbia University Press, 1990, p. 254.
17. Nishioka, T. and Mualchin, L., Structural Eng./Earthquake Eng., Japan Society of Civil Engineering, no. 570/I–40, 1997.
18. Mualchin, L., Technical Report to accompany the Caltrans California Seismic Hazard Map 1996, (based on maximum credible earthquakes), California Department of Transportation, Sacramento, 1996, pp.57.
19. Greensfelder, R. W., California Division of Mines and Geology, Map Sheet 23, 1974.
20. Mualchin, L. and Jones, A. L., DMG Open-File Report 92-1, California Dept of Conservation, Division of Mines and Geology, Sacramento, CA, 1992.

21. Husband, J. J., Report No. EDD 76-1, Engineering Geology and Foundation Section, Nevada State Highway Department, Carson City, NV, 1976.
22. Siddharthan, R., Anderson, J. G., Bell, J. and dePolo, C. M., Final Report to the Nevada Department of Transportation, Department of Civil Engineering, Nevada Bureau of Mines and Geology, and Seismological Laboratory, University of Nevada, Reno, 1993.
23. Nuttli, O. W., *Reviews of Engineering Geology* (eds. Hathaway, A. W. and McClure, C. R.), Geol. Soc. Am., 1979, vol. 4, pp. 67–94.
24. Anderson, J. G., *Eng. Geol.*, 1997, **48**, 43–57.
25. Special Publication 61, California Department of Conservation and Division of Mines and Geology, Sacramento, CA, 1982.
26. Report, Risk Management Solutions Inc., Menlo Park, CA, 1995.
27. dePolo, C. M., Rigby, J. G., Johnson, G. L., Anderson, J. G. and Wythes, T. J., Spl Publ. 20, Nevada Bureau of Mines and Geology, 1996.
28. Anderson, J. G. and Brune, J. N., *Seismol. Res. Lett.*, 1998, **69**, 71.
29. Anderson, J. G. and Brune, J. N., *Seismol. Res. Lett.*, 1999, **70**, 19–28.
30. Wesnousky, S. G., *J. Geophys. Res.*, 1986, **91,** 12587–12631.
31. Stirling, M. W., Ph D thesis, University of Nevada, Reno, May 1998.
32. Senior Seismic Hazard Analysis Committee (SSHAC), NUREG/CR-6372, US Nuclear Regulatory Commission, Washington, DC 20555, 1997.
33. Panel on Seismic Hazard Evaluation, Review of Recommendations for Probabilistic Seismic Hazard Analysis: Guidance on Uncertainty and Use of Experts, National Academy Press, Washington, DC, 1997, pp. 73.
34. Abrahamson, N. A. and Silva, W. J., *Seismol. Res. Lett.*, 1997, **68**, 94–127.
35. Zeng, Y., Anderson, J. G. and Yu, G., *Geophys. Res. Lett.*, 1994, **21,** 725–728.
36. Working Group on California Earthquake Probabilities (WGCEP), *Bull. Seismol. Soc. Am.*, 1995, **85,** 379–439.
37. Atkinson, G. M. and Boore, D. M., *Seismol. Res. Lett.*, 1997, **68**, 24–40.
38. Toro, G. W., Abrahamson, N. A. and Schneider, J. F., *Seismol. Res. Lett.*, 1997, **68,** 41–57.
39. Youngs, R. R., Chou, S. J., Silva, W. J. and Humphrey, J. R., *Seismol. Res. Lett.*, 1997, **68**, 58–73.
40. Boore, D. M., Joyner, W. B. and Fumal, T. E., *Seismol. Res. Lett.*, 1997, **68**, 128–153.
41. Campbell, Kenneth W., *Seismol. Res. Lett.*, 1997, **68,** 154–179.
42. Sadigh, K., Chang, C. Y., Egan, J. A., Makdisi, F. and Youngs, R. R., *Seismol. Res. Lett.*, 1997, **68**, 180–189.
43. Spudich, P., Fletcher, J. B., Hellweg, M., Boatwright, J., Sullivan, C., Joyner, W. B., Hanks, T. C., Boore, D. M., McGarr, A., Baker, L. M. and Lindh, A. G., *Seismol. Res. Lett.*, 1997, **68,** 190–198.
44. Anderson, J. G., *Bull. Seismol. Soc. Am.*, 2000 (in press).
45. Ni, S., Anderson, J. G., Zeng, Y. and Siddharthan, R., *Bull. Seismol. Soc. Am.*, 2000 (in press).
46. Field, E. H., Kramer, S., Elgemal, A. W., Bray, J. D., Matasovic, N., Johnson, P. A., Cramer, C., Roblee, C., Wald, D., Bonilla, L. F., Dimitriu, P. P. and Anderson, J. G., *Seismol. Res. Lett.*, 1998, **69,** 230–234.
47. Chin, B. H. and Aki, K., *Bull. Seismol. Soc. Am.*, 1991, **81,** 1859–1884.
48. Su, F., Anderson, J. G. and Zeng, Y., *Bull. Seismol. Soc. Am.*, 1998, **88,** 1411–1425.
49. Field, E. H. and the Phase III Working Group, *Bull. Seismol. Soc. Am.*, 2000 (in press).
50. Field, E. H., *Bull. Seismol. Soc. Am.*, 2000 (in press).
51. Field, E. H. and Peterson, M. D., *Bull. Seismol. Soc. Am.*, 2000 (in press).
52. Lee, Y., Anderson, J. G. and Zeng, Y., *Bull. Seismol. Soc. Am.*, 2000 (in press).
53. Lee, Y. and Anderson, J. G., *Bull. Seismol. Soc. Am.*, 2000 (in press).
54. Olsen, K. B., *Bull. Seismol. Soc. Am.*, 2000 (in press).
55. Steidl, J. H., *Bull. Seismol. Soc. Am.*, 2000 (in press).
56. Tinsley, J. C. and Fumal, T. E., US Geol. Surv. Profess. Paper 1360, 1985, pp. 101–126.
57. Wills, C. J., Petersen, M., Bryant, W. A., Reichle, M., Saucedo, G. J., Tan, S., Taylor, G. and J. Treiman, *Bull. Seismol. Soc. Am.*, 2000 (in press).
58. Magistrale, H., Day, S. and Clayton, R., *Bull. Seismol. Soc. Am.*, 2000 (in press).
59. Joyner, W. B., *Bull. Seismol. Soc. Am.*, 2000 (in press).
60. Lee, Y., Zeng, Y. and Anderson, J. G., *Bull. Seismol. Soc. Am,* 1998, **88,** 291–296.
61. Anderson, J. G. and Yu, G., *Bull. Seismol. Soc. Am.*, 1996, **86,** S100–S114.
62. US Geological Survey, USGS Circular 1193, Denver, Colorado, 2000.
63. Anderson, J. G., Sucuoglu, H., Erberik, A., Yilmaz, T., Durukal, E., Erdik, M., Anooshehpoor, R., Brune, J. N. and Ni, S. -D., *Earthq. Spectra,* 2000 (in press).
64. Shin, T. C., Kuo, K. W., Lee, W. H. K., Teng, T. L. and Tsai, Y. B., *Seismol. Res. Lett.*, 2000, **71,** 24–30.
65. Kao, H. and Chen, W. P., *Science,* 2000, **288,** 2346–2349.
66. Somerville, P. G., Smith, N. F., Graves, R. W. and Abrahamson, N. A., *Seismol. Res. Lett.*, 1997, **68**, 199–222.
67. Anderson J. G. and Lei, Y., *Bull. Seismol. Soc. Am.*, 1994, **84,** 1003–1017.
68. Anderson, J. G., *Seismol. Res. Lett.*, 1997, **68**, 86–93.
69. Paul Somerville (pers. commun.)
70. Wesnousky, S. G., *Nature,* 1989, **335,** 340–343.
71. Ni, S., Brune, J. N. and Anderson, J. G., *Seismol. Res. Lett.*, 2000, **71,** 225.
72. Brune, J. N., *Seismol. Res. Lett.*, 1999, **70,** 29–33.
73. Brune J. N., *Bull. Seismol. Soc. Am.*, 2000 (submitted).
74. Ni, S., Anderson, J. G. and Zeng, Y., *Seismol. Res. Lett.*, 2000, **71,** 230.
75. Brune, J. N., *Bull. Seismol. Soc. Am.*, 1996, **86**, 43–54.
76. Shi, B., Anooshehpoor, A., Brune, J. N. and Zeng, Y., *Bull. Seismol. Soc. Am.*, 1998, **88,** 1484–1494.
77. Anooshehpoor, A., Heaton, T. H., Shi, B. and Brune, J. N., *Bull. Seismol. Soc. Am.*, 1999, **89**, 845–853.
78. Anooshehpoor, A., Brune, J. N. and Zeng, Y., *Seismol. Res. Lett.*, 2000, **71**, 263.
79. Anooshehpoor, A. and Brune, J. N., *Bull. Seismol. Soc. Am.*, 2000 (submitted).
80. Brune, J. N., *Proc. Indian Acad. Sci. (Earth Planet. Sci.)*, 1996, **105,** L197–L206.
81. Brune, J. N. and Anooshehpoor, A., *Bull. Seismol. Soc. Am.*, 1998, **88,** 1070–1078.
82. Ogelsby, D. D., Archuleta, R. J. and Nielsen, S. B., *Science*, 1998, **280,** 1055–1059.
83. Shi, B., Ph D thesis, Department of Geological Sciences, University of Nevada, Reno, 1999.
84. Ely, G. P. and Day, S. M., *Seismol. Res. Lett.*, 2000, **71,** 267.
85. Ogelsby, D. D., Archuleta, R. J. and Nielsen, S. B., *Bull. Seismol. Soc. Am.*, 2000, **90,** 616–628.
86. Allen, C. R., Brune, J. N., Cluff, L. S. and Barrows, A. G. Jr., *Seismol. Res. Lett.*, 1998, **69**, 524–532.
87. Oldham, R. D., *Mem. Geol. Surv. India*, 1899, **29**, 379.
88. Nason, R. D., Report, US Dept. of Commerce, Washington, 1973, pp. 123–126.
89. Iida, K., *Selected Scientific Papers of Prof. Kumiji Iida* (in Japanese), Disaster Prevention Res. Lab., Fac. Eng., Aichi Eng. Univ., 1985, pp. 570–668.

90. Brune, J. N., Proceedings and Abstracts, SCEC Annual Meeting, Palm Springs, California, 26–29 September 1999, p. 51.
91. Dunbar, W. S., Boore, D. M. and Thatcher, W., *Bull. Seismol. Soc. Am.*, 1980, **70,** 1893–1905.
92. Bawden, G. W., Donnellan, A., Kellog, L. H., Dong, D. and Rundle, J. B., *J. Geophys. Res.*, 1997, **102,** 4957–4967.
93. Bawden, G. W., *J. Geophys. Res.*, 2000 (submitted).
94. Oakeshott, G. B. (ed.), Bulletin 171 of the California Division of Mines, 1995.
95. McGill, S. F., Grant, D. and Wells, S. G., Southern California Earthquake Center, Annual Meeting Abstracts, 1998, pp. 76–77.
96. Anderson, J. G. and Luco, J. E., *Bull. Seismol. Soc. Am.*, 1983, **73**, 23–43.
97. Mendez, A. J. and Luco, J. E., *J. Geophys. Res.*, 1988, **93**, 12041–12054.
98. McGarr, A., Fletcher, J. B. and Harris, R. A., *Seismol. Res. Lett.*, 2000, **71**, 265.
99. Wills, C. J. and Borchardt, G., *Geology,* 1993, **21,** 853–856.
100. Anderson, J. G. and Brune, J. N., Proceedings, 12th World Conference on Earthquake Engineering, Auckland, New Zealand, 31 Jan.–4 Feb. 2000.
101. Sanders, C. O. and Kanamori, H., *J. Geophys*., 1984, **89**, 5873–5890.
102. Brune, J. N. and Anooshehpoor, A., *J. Geophys. Res.*, 1999, **104**, 809–815.
103. Shi, B., Y. Zeng and Brune, J. N., *Seismol. Res. Lett.*, 1997, **68**, 333.
104. Ramelli, A. R., dePolo, C. M. and Bell, J. W., Report, Nevada Bureau of Mines and Geology, University of Nevada, Reno, 1994.
105. Ramelli, A. R., 1999 (pers. commun).
106. Bryant, W. A., CDMG Open-File report 84-56 SAC, Plate 1, 1984.
107. Jennings, C. W., DMG Open-File Report 92-03, 1992.
108. Spudich, P., Joyner, W. B., Lindh, A. G., Boore, D. M., Margaris, B. M. and Fletcher, J. B., *Bull. Seismol. Soc. Am.*, 1999, **89**, 1156–1170.
109. Westaway, R. and Smith, R. B., *Geophys. J.*, 1989, **96**, 529–559.
110. Brune, J. N., Johnson, P. and Slater, C., *J. Himalayan Geol.*, 1990, **1**, 155–166.
111. Brune, J. N., Brown, S. and Johnson, P., *Tectonophysics*, 1993, **218**, 59–67.
112. Anooshehpoor, A. and Brune, J. N., *PAGEOPH*, 1994, **142**, 735–747.

ACKNOWLEDGEMENTS. This research was supported by NSF CMS 9528517, USGS 1434-HQ-97GR03045 and the Southern California Earthquake Center. SCEC is funded by NSF Cooperative Agreement EAR-8920136 and USGS Cooperative Agreements 14-08-0001-A0899 and 1434-HQ-97AG01718. The SCEC contribution number for this paper is 532.